PROCEEDINGS OF SCIENCE

Highlights from ANTARES, and prospects for KM3NeT

Clancy W. James*
ECAP, University of Erlangen-Nuremberg
E-mail: clancy.james@physik.uni-erlangen.de
on behalf of the ANTARES and KM3NeT Collaborations

The ANTARES experiment has been running in its final configuration since 2008. It is the largest neutrino telescope in the Northern hemisphere. After the discovery of a cosmic neutrino diffuse flux by the IceCube detector, the search for its origin has become a key mission in high-energy astrophysics. Particularly interesting is the indication (although not significant with the present IceCube statistics) of an excess of signal events from the Southern sky region.
The ANTARES sensitivity is large enough to constrain the origin of the IceCube excess from regions extended up to 0.2 sr in the Southern sky. Assuming different spectral indices for the energy spectrum of neutrino emitters, the Southern sky and in particular central regions of our Galaxy are studied searching for point-like objects, for extended regions of emission, and for signal from transient objects selected through multimessenger observations. For the first time, cascade events are used for these searches, using a new method with 3° angular resolution.
ANTARES has also provided results on searches for rare particles (such as magnetic monopoles and nuclearites in the cosmic radiation), and multi-messenger studies of the sky in combination with different experiments. Of particular note are the searches for Dark Matter: the limits obtained for the spin-dependent WIMP-nucleon cross section overcome that of existing direct-detection experiments.
The contribution concludes with an outlook to the next-generation experiment KM3NeT, which is already under construction. KM3NeT will consist of two components: ORCA, optimised for measuring atmospheric neutrino oscillation parameters in the few-GeV range; and ARCA, for studying astrophysical neutrinos at higher energies. The status of KM3NeT will be summarised and the resulting prospects for ORCA and ARCA discussed.

The 34th International Cosmic Ray Conference,
30 July- 6 August, 2015
The Hague, The Netherlands

*Speaker.

PoS(ICRC2015)024

1. Introduction

The underwater neutrino telescope ANTARES has been operating in its final configuration since 2008. Anchored to the seabed at a depth of 2.5 km, and located 40 km off the coast of Toulon, France, it is the largest neutrino telescope in the Northern Hemisphere. Consisting of an array of 885 $10''$ photomultiplier tubes covering an instrumented volume of approximately 0.01 km^3, it is designed primarily to search for $E \gtrsim 100$ GeV muons resulting from the charged-current interactions of ν_μ in the vicinity of the detector.

Highlights from a wide range of analyses using ANTARES data are reported here. These include several measurements which are used to constrain both point-like (Sec. 2) and extended (Sec. 4) origins of the astrophysical flux observed by IceCube [2, 3, 4], and a new cascade reconstruction method which, due to its high angular resolution, for the first time allows a point-source search with cascade events (Sec. 3). Updated limits on dark matter are also given in Sec. 5).

ANTARES is planned to cease operation in 2017. At the same time, Phase 1 of the next-generation instrument KM3NeT will be completed. With a flexible block design, KM3NeT will be deployed in both a compact configuration ('ORCA') to study neutrino oscillations and the neutrino mass hierarchy, and a sparser configuration ('ARCA') for performing high-energy neutrino astronomy. The status of KM3NeT deployment, and the prospects for ARCA and ORCA during Stage 2 of KM3NeT, is given in Sec. 6.

2. Searches for astrophysical neutrino point sources

The main channel by which ANTARES searches for astrophysical point-like sources of neutrinos is by searching for an excess of energetic μ from the interactions of ν_μ in the vicinity of the detector. The high rate of downgoing μ from the interactions of cosmic rays (CR) in the Earth's atmosphere restricts such searches to events coming from below, or only a few degrees above, the horizon. The primary background to such searches then becomes the flux of atmospheric ν_μ, and those few atmospheric μ events mis-reconstructed as up-going. The long scattering length of blue light in seawater provides an excellent directional resolution on the ν_μ primary of 0.38° for an E^{-2} source [6], which is tested using the Moon shadow (M. Sanguineti, ICRC2015 1138). This allows a very strong suppression of both backgrounds, and a correspondingly good sensitivity to neutrino sources from the Southern Hemisphere. Its ability to probe the origin of the IceCube astrophysical flux is best-characterised through the joint analysis described below. Throughout, flavour-uniform spectra are assumed, consistent with observations [4].

2.1 Joint analysis with IceCube

A joint analysis using ANTARES and IceCube data is detailed in Barrios-Martí & Finley (ICRC2015 1076). The fractional number of source events expected to be present in each data set is shown in Fig. 1 (left) for an $E^{-2.5}$ spectra, the current best-fit to the IceCube flux. The fraction of events contributed by the ANTARES sample is greater for $\delta \lesssim 15^\circ$, where ANTARES is more sensitive to low-energy upcoming muon tracks, while IceCube requires high-energy events to distinguish them from the down-going muon background. The sensitivity is also a function of the background rates, and angular and energy resolutions, which are not shown.

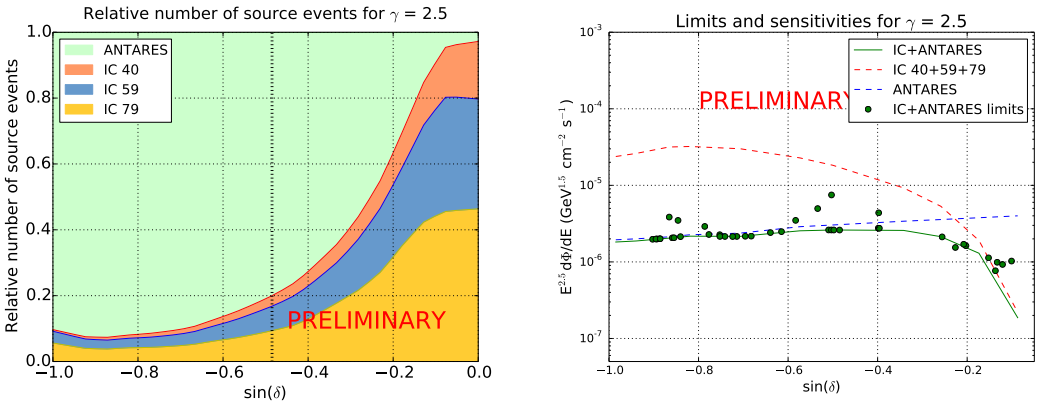

Figure 1: Left: Fractional contributions of each data set to the total number of signal events passing cuts in the joint ANTARES–IceCube analysis (Barrios-Martí & Finley, ICRC2015 1076), for sources with an $E^{-2.5}$ spectrum, as a function of declination δ. Right: Sensitivities (lines) and limits (dots) to an $E^{-2.5}$ flux with no cutoff, using ANTARES (blue), IceCube (red), and combined (green) data, as a function of δ.

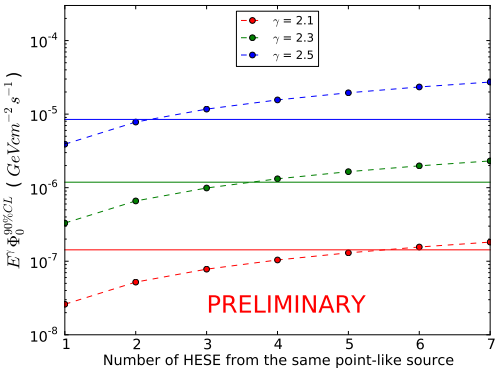

Figure 2: ANTARES limits (solid lines) at 90% C.L. on the contribution of point-like sources to the IceCube HESE sample [3] for different spectral indices, shown for a source at $\delta = -29°$. (J. Barrios-Martí, ICRC2015 1077). These are compared to (dashed lines) the flux required to produce a given expected number of HESE [5]. The result is similar for other declinations around the Galactic Centre.

The results of the combined search are shown in Fig. 1 (right), for an $E^{-2.5}$ source spectrum. No significant cluster is found, with the most significant source on the candidate list being 3C 279, with a pre-trial p-value of 0.05. Over the entire Southern sky, the combined analysis improves on the results from both experiments, indicating the complementarity of the two instruments.

2.2 Limits on point-source origins of the HESE

It has been proposed [7] that the cluster of IceCube events seen in Ref. [3] could be due to a single point-like source, which is not detectable due to the low angular resolution. The non-detection of an ANTARES point-like source in this region, as reported by J. Barrios-Martí (ICRC2015 1077), limits the flux of such a source as a function of spectral index, shown by the solid lines and y-axis of Fig. 2. The flux required to produce a given number of events in the HESE analysis (x-axis) is also shown. The range where the latter is greater than the former rules out a corresponding contribution from any single point-like source with that spectral index at 90% confidence level (C.L.).

The result above is particularly relevant because the current best-fit spectrum (between 25 TeV and 2.8 PeV) of the IceCube flux has a spectral index of -2.50 ± 0.09 [4]. ANTARES can thus rule

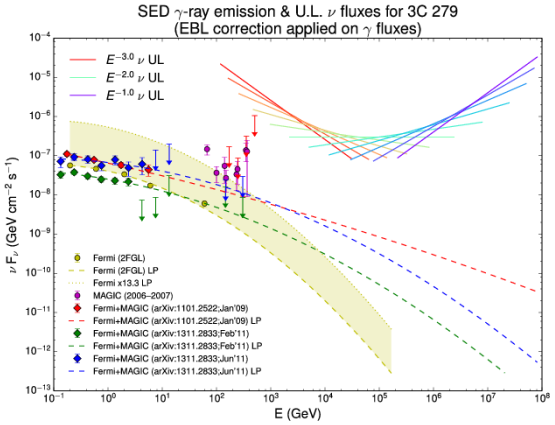

Figure 3: Result from time-dependent analyses using gamma-ray data. Limits on the neutrino flux from the blazar 3C 279 as a function of spectral index (solid lines; Sánchez-Losa & Dornic, ICRC2015 1075), compared to the observed (points) and extrapolated (dashed lines) gamma-ray spectra observed by *Fermi* and IACTs.

out any single point-source of neutrinos in the region of the Galactic Centre with spectral index of -2.5 as having a flux corresponding to more than 2 HESE.

2.3 Flares from AGN and X-ray binaries

AGN have long been proposed as a source of high-energy cosmic rays and, hence, neutrinos [8]. Blazars, being active galactic nuclei with jets pointed towards the line-of-sight, exhibit bright flares which dominate the extragalactic γ-ray sky observed by *Fermi*-LAT [9].

Using multi-wavelength observations, several bright blazars have been reported by the TANAMI collaboration [10] to lie within the 50% error bounds of the reconstructed arrival directions of the PeV-scale events IC 14 and IC 20 observed by IceCube [3]. As discussed by Kadler et al. (ICRC2015 1090), ANTARES observes signal-like events from the two brightest blazars, both in the field of IC 20 [11], although this is also consistent with background fluctuations. A lack of such events from the field of IC 14 excludes a neutrino spectrum softer than $E^{-2.4}$ as being responsible for this event. The highest-energy 'Big Bird' event (IC 35) was detected during an extremely bright flare from the blazar PKS B1424-418, which lies within the 50% error region of the IC 35 arrival direction. ANTARES finds only one event within 5° of this source during the flaring period, whereas approximately three would be expected from random background fluctuations alone.

In another analysis (Sánchez-Losa & Dornic, ICRC2015 1075), ANTARES targets a sample of 41 blazar flares observed by *Fermi* LAT and 7 by the IACTs H.E.S.S., MAGIC, and VERITAS. The lowest pre-trial p-value of 3.3% was found for the blazar 3C 279, which comes from the coincidence of one event with a 2008 flare previously reported by Ref. [12]. However, the post-trial p-value is not significant. The resulting limits are given in Fig. 3.

Similar methods were also used to search for neutrino emission during the flares from galactic x-ray binaries (Dornic & Sánchez-Losa, ICRC2015 1046). A total of 34 x-ray- and γ-ray-selected binaries were studied, with no significant detections, allowing some of the more optimistic models for hadronic acceleration in these sources to be rejected at 90% C.L..

2.4 Gamma-ray bursts

Long-duration gamma-ray bursts (GRBs) have been proposed as a source of the highest-energy cosmic rays [13]. ANTARES searches for a neutrino flux from GRBs considering two methods of

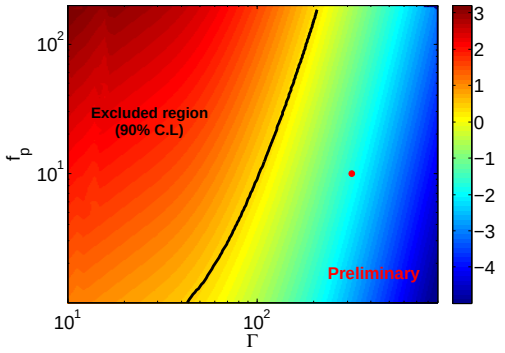

Figure 4: Range of jet Γ-factor and baryonic loading f_p excluded by ANTARES in the case of GRB110918A using the NeuCosmA model of Ref. [14], as described by Schmid & Turpin (ICRC2015 1057). The assumed values of $\Gamma = 316$ and $f_p = 10$ are shown by the red point, while the colour-coding gives the expected number of observable neutrinos. The predicted ν emission scales with Γ^{-5} and linearly with f_p.

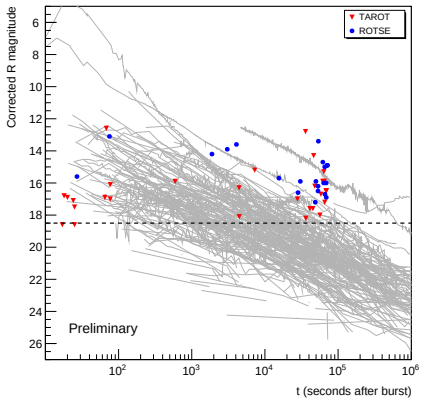

Figure 5: Points: limiting magnitudes and delay times of optical follow-up observations to ANTARES alerts with ROTSE and TAROT (A. Mathieu, ICRC2015 1093) compared to (grey lines) the light-curves from measured GRBs.

modelling emission processes: the NeuCosmA description of Ref. [14], and the 'photospheric' model of Ref. [15]. In each case, the expected signal is simulated on a burst-by-burst basis, and the detector response and background are modelled using the exact oceanic conditions at the time of the burst. The ANTARES analysis using the NeuCosmA model was developed and applied to a sample of 296 bursts in Ref. [16], with no coincident neutrino events detected. Since then, one especially powerful burst GRB110918A, and the nearby burst GRB130427A, have been identified as promising candidates for neutrino detection, and studied in detail by Schmid & Turpin (ICRC2015 1057). No coincident events are observed from either burst, with limits set on the bulk gamma-factor and baryonic loading of the jet, as shown in Fig. 4.

A search using the photospheric models is developed by M. Sanguineti (ICRC2015 1068), and will shortly be unblinded. The GRB search methods are also being extended to test Lorentz invariance violation (Schmid & Turpin, ICRC2015 1057), which would delay the arrival times of TeV neutrinos compared to GeV photons.

2.5 Optical and X-ray follow-up

The TAToO (telescopes–ANTARES target-of-opportunity) program [17] performs near-real-time reconstruction of muon-track events. If a sufficiently high energy event is reconstructed as coming from below the horizon (i.e. those events most likely to be of astrophysical origin), an alert message is generated to trigger robotic optical telescopes, and, with a higher threshold, the *Swift*-XRT. The very short alert-generation time (a few seconds) and half-sky simultaneous cover-

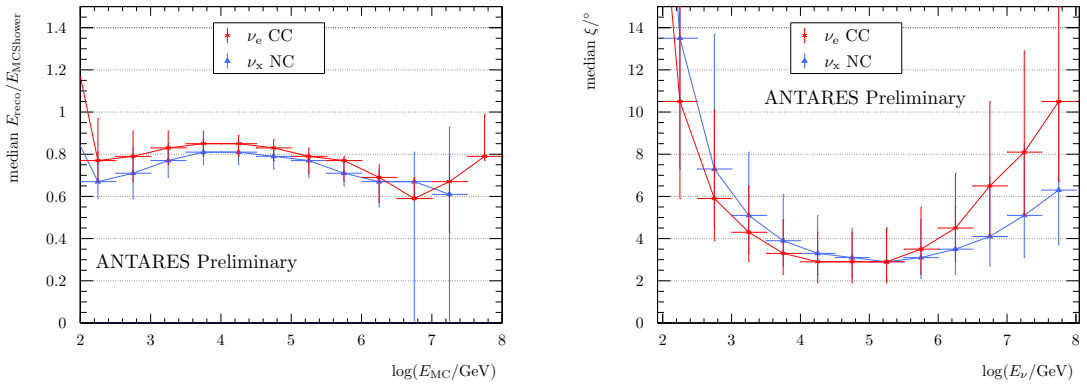

Figure 6: Energy (left) and angular (right) resolutions for ν_μ and ν_e NC (blue), and ν_e CC (red), events with ANTARES (T. Michael, ICRC2015 1078).

age of ANTARES makes it ideal for detecting transient signals, and optical and x-ray follow up observations have been initiated within 20 s and one hour respectively.

Result from 42 optical and 7 x-ray alerts are reported by A. Mathieu (ICRC2015 1093). While no associated transient event was detected, this non-observation can be used to place limits on the astrophysical origin of the detected neutrinos (A. Mathieu, ICRC2015 1093), as shown in Fig. 5. The steep fall-off of the light-curves emphasises the need for a rapid alert generation and follow-up: observations within one minute can rule out a GRB origin with high confidence, while those after one day would be unlikely to detect even a bright GRB.

3. Cascades

The effective area of neutrino telescopes such as ANTARES and IceCube to cascade events (neutral-current (NC) interactions, and ν_μ and ν_τ charged-current (CC) interactions) is generally lower than to ν_μ CC interactions, due to the very long range of the outgoing μ. Additionally, the angular resolution to through-going μ is superior. However, the cascade channel has several advantages: neutrino events are more easily distinguished from the background of atmospheric muons, allowing both up- and down-going events to be studied; and the energy deposited in the detector is more-strongly correlated with the energy of the neutrino primary. It was these latter advantages that allowed the diffuse cosmic neutrino flux detected by IceCube to be first observed in the cascade channel [2].

Cascade event identification and reconstruction has been in development in ANTARES for several years, and its application in a search for a diffuse flux is reported below. The most important development however has been a new cascade reconstruction algorithm with an unprecedented angular resolution, of typically 3° accuracy, which for the first time enables a point-source search using the cascade channel.

3.1 Cascade reconstruction in ANTARES

The most recent cascade-reconstruction algorithm developed for ANTARES, reported by T. Michael (ICRC2015 1078), is termed ‘Tantra’. Its performance is shown in Fig. 6. Over the approximate

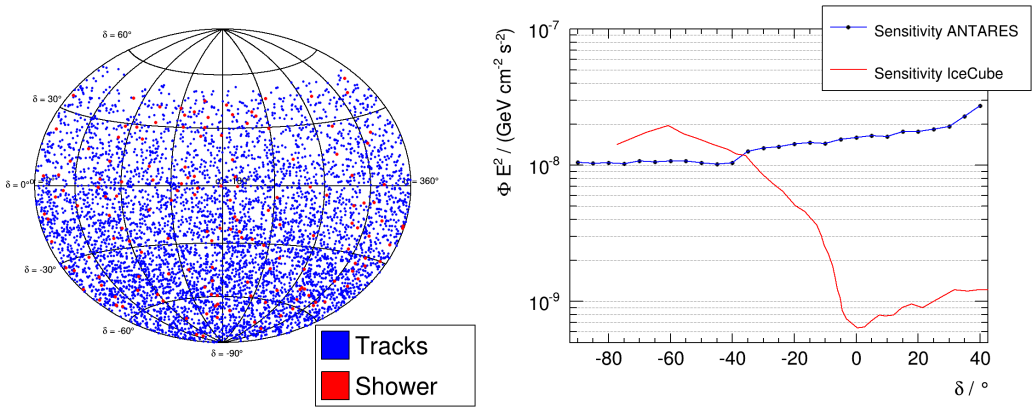

Figure 7: Left: The arrival directions of events used in the ANTARES all-sky point-source-search sample. Right: sensitivity of the ANTARES targeted search to flavour-uniform neutrino point sources with E^{-2} spectra in terms of flux per flavour, compared to the IceCube results from Ref. [4].

10-300 TeV range, arrival directions are reconstructed with a median angular error of 3°, and a resolution on deposited energy of 5% (the offset from $E_{\rm reco}/E_{\rm MC} = 1$ is easily corrected for), although the latter is limited by the total ANTARES systematic energy uncertainty of approximately 10%. Below 10 TeV, the resolutions worsen due to a decreasing number of photons being detected, while above 300 TeV, the events begin to saturate the detector. Over the entire 100 GeV to 100 PeV range, the median angular resolution improves on the IceCube resolution for purely shower-like high-energy starting events (i.e. those without an outgoing muon) [3].

3.2 Point-source search including cascades

A combined point-source search using both muon-track and cascade events has been performed using 1622 days of effective livetime from 2007 to 2013 (T. Michael, ICRC2015 1078). After cuts, the sample consisted of 6261 muon-track events, and 156 cascade events, with an estimated contamination of 10% mis-reconstructed atmospheric muons in each.

The resulting skymap is shown in Fig. 7 (left). An untargeted point-source search, a search over a list of pre-specified candidates, and a search using the origins of the IceCube events reported in Ref. [3] were applied to this data. No significant excess was observed. The resulting limits on point-like sources are given in Fig. 7 (right). While the atmospheric background produces predominantly muon-track events, an E^{-2} point source with a flavour-uniform flux would be expected to produce a cascade-to-track ratio of 3:10, significantly increasing the sensitivity of the search. Thus the achieved search sensitivity was approximately 10^{-8} GeV^{-1} cm^{-2} s^{-1} for $\delta < -40°$.

3.3 Diffue flux search

A diffuse flux search in ANTARES has been developed that makes optimal uses of both muon-track and cascade events (Schnabel & Hallmann, ICRC2015 1065). Since any explicit selection of muon-like and cascade-like events inevitably discards events with topologies falling between the two classes, no such selection was made.

The procedure was first optimised for, and applied to, the 913 days of effective livetime between 2007 and 2013 exhibiting the best data-taking conditions (mostly low bioluminescent ac-

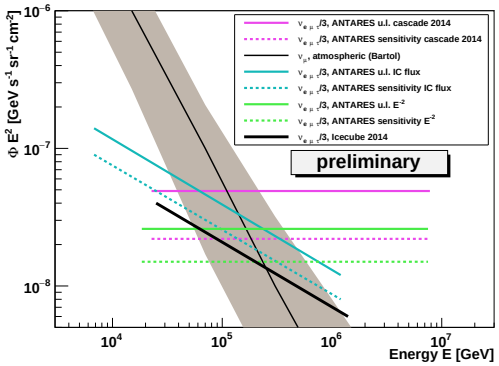

Figure 8: ANTARES sensitivity to (dotted), and limits on (solid), a diffuse astrophysical neutrino flux (Schnabel & Hallmann, ICRC2015 1065), showing (pink) the previous ANTARES limit [20], (green) this work, and (blue) the flux observed by IceCube [4]. This is compared to the conventional atmospheric background flux (black) [18], with associated error (grey shading).

tivity). The expected number of events from the standard and prompt atmospheric background [18, 19] was 9.5 ± 2.5, composed of 5.5 ν_μ CC, 1 atmospheric μ, and 2.9 ν NC and ν_e events. The expectation from the IceCube neutrino flux reported by Ref. [4][1] was 5.0 ± 1.1 events.

After unblinding, 12 events passed the selection cuts — consistent with both background-only, and background and IceCube diffuse flux expectations. The resulting limits on an E^{-2} flux are given in Fig. 8.

4. Extended source searches

In addition to the numerous point-like candidate neutrino sources targeted in Secs. 2 and 3, several extended regions have been proposed as hadronic acceleration sites. ANTARES searches for an excess neutrino flux from these regions using 'on-zones' defined by specific templates, which are compared to 'off-zones' of exactly the same size and shape, but offset in right ascension. Thus the off-source regions give an unbiased estimate of the background in the source region in a way that is independent of simulations. Results for the Fermi Bubbles, Galactic plane, and the IceCube cluster are described below.

4.1 Fermi bubbles

The Fermi Bubbles [21] are giant regions of γ-ray emission extending out of the galactic centre, and are proposed hadronic acceleration site [23], with neutrinos expected from p–p collisions. A first search in ANTARES data from 2008–2011 for emission from these regions was presented by Ref. [22] — here, an update is presented using 2012–2013 data.

The on- and off-zone regions used in the Fermi Bubble analysis are shown in Fig. 9 (left). Flavour-uniform E^{-2} and $E^{-2.18}$ neutrino fluxes are assumed, where the latter is motivated by the best-fit proton spectrum of $E^{-2.25}$ reported by Ref. [23]. Exponential cut-offs at energies of 500, 100, and 50 TeV are also tested.

A slight excess is found in the source region, corresponding to a 1.9 σ significance. The corresponding upper limits on an $E^{-2.18}$ neutrino flux are compared in Fig. 9 (right) to the expectations from Ref. [23].

[1] Flux-per-flavour of $\Phi = 2.23 \times 10^{-18} (E/1\text{TeV})^{-2.5}$ GeV^{-1} cm^{-2} s^{-1} sr^{-1}

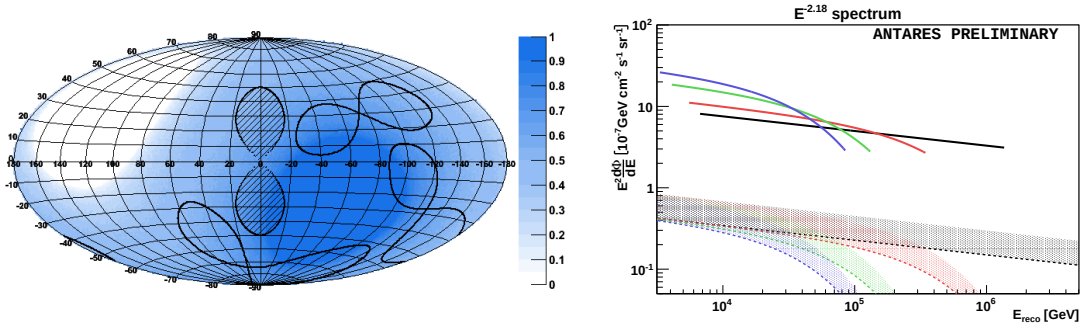

Figure 9: Left: on- and off-zone search regions for the Fermi Bubble search of S. Hallmann (ICRC2015 1059), compared to the ANTARES visibility (blue shading). Right: 90% C.L. upper limits (lines) on the neutrino flux from the Fermi Bubbles, compared to (shaded regions) expectations [23] for different spectral shapes.

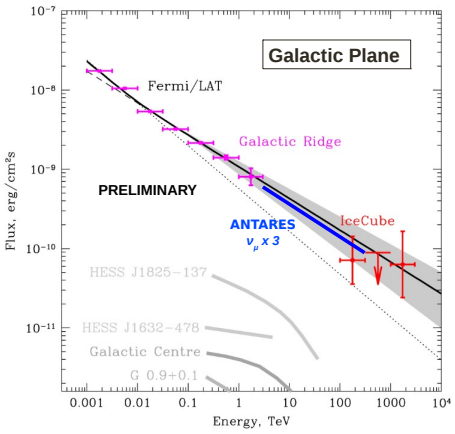

Figure 10: *Fermi*-LAT-detected gamma-ray flux from the Galactic Ridge (pink), and IceCube events consistent with this region (red), as computed in Ref. [24], compared to the ANTARES all-flavour flux limit (blue) (L. Fusco, ICRC2015 1055) and gamma-ray fluxes from various other galactic sources (grey) [25].

4.2 Galactic plane

Cosmic rays in our galaxy will collide with the interstellar medium to produce pions and, hence, neutrinos. Direct evidence for these processes comes from observations by *Fermi*-LAT [26] of the diffuse galactic γ-ray background. It is also interesting that the number of IceCube high energy starting events (HESE) in the $E > 100$ TeV range [3] with angular reconstructions consistent with this region corresponds to a flux consistent with that observed in γ rays [24], as shown in Fig. 10. The large uncertainty in the arrival directions of cascade-like HESE, and their low number, makes this comparison difficult however. More-detailed simulations of the expected neutrino flux are given in Refs. [25].

ANTARES' northern latitude is ideally suited to studying the expected neutrino flux from the inner galactic plane, and a search has been performed searching in the regions of galactic longitude $|l| < 40°$ and latitude $|b| < 3°$, as reported by L. Fusco (ICRC2015 1055). The search used nine off-zones and one on-zone, and found no excess in the on-zone region (one event compared to an average of 2.5 for the off-zones). The resulting limits are shown in Fig. 10. In particular, the hypothesis of a 1–1 relation between the γ-ray and neutrino flux from the Galactic Ridge is ruled out at 90% confidence, showing that ANTARES is already testing the well-established multimessenger γ–ν–CR paradigm in our galaxy. The limits cannot rule out however models from more-detailed

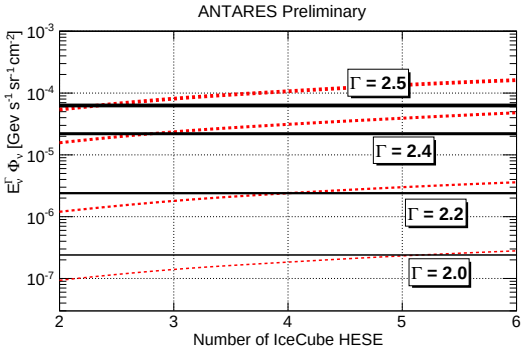

Figure 11: ANTARES upper limits at 90% C.L. (black) on a flavour-uniform neutrino flux from the IceCube cluster region as a function of the spectral index Γ, compared to (red) the flux required to produce an expected number of events in the IceCube HESE analysis [5]. The maximum number of IceCube events allowed at 90% C.L. is indicated by the crossing points of the red and black lines for a given spectral index. See L. Fusco (ICRC2015 1055) for details.

simulations of galactic cosmic-ray propagation.

4.3 IceCube cluster

The same search techniques employed in the galactic plane search were used to probe the origin of the cluster of IceCube events seen in Ref. [3]. The analysis (L. Fusco, ICRC2015 1055) used twelve off-zones and one on-zone to search for an excess of events. One event passing selection cuts is observed in both the on-zone and the average off-zone, i.e. no excess (significant or otherwise) is observed. Resulting limits on the maximum number of HESE produced by a source with different spectral indices are presented in Fig. 11, calculated analogously to the point-source search of Sec. 2 and Fig. 2. For the best-fit IceCube diffuse spectral index $\Gamma = 2.5$ [4], ANTARES rejects at 90% confidence a flux from this region expected to produce three or more of the IceCube events in the cluster. This extends the results of Ref. [6] and J. Barrios-Martí (ICRC2015 1077) for this region, which limit the existence of point-like and mildly extended sources in this region.

4.4 Model-independent searches

It is possible that as-yet unknown sources or source populations produce a significant neutrino flux. Two techniques have been used by ANTARES to perform the most general searches possible. A two-point autocorrelation analysis is performed by R. Gracia Ruiz (ICRC2015 1074), searching for an excess of clustering on angular scales up to 60°. A small (2.2σ) excess is found at angular scales of less than 0.5°, i.e. within the reconstruction accuracy of the detector, though this is not statistically significant.

In S. Geißelsöder (ICRC2015 1054), a search for individual sources of arbitrary shape and size is presented. The algorithm searches for local clustering, and identifies regions with an excess of events. This procedure identified a very large structure of unusual shape containing the galactic centre region, with a post-trial p-value of 2.5σ based on simulations and data-scrambling. A detailed analysis of possible systematic effects has not identified any reason for such a fluctuation, and the correct interpretation of this result remains an open question.

5. Dark matter and Exotics

ANTARES can place limits on different WIMP dark-matter scenarios by limiting the neutrino flux expected from WIMP interactions in the Sun, Earth, Galactic Centre, and dwarf galaxies.

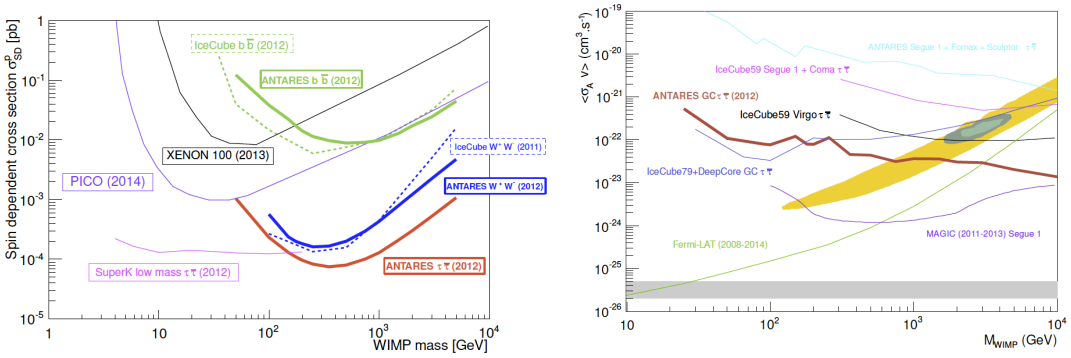

Figure 12: ANTARES limits σ^p_{SD} from the Sun (left) and on $\langle\sigma_A v\rangle$ from the Galactic Centre (right) as a function of the WIMP mass. See C. Tönnis (ICRC2015 1207) for details and associated references.

Since the expected dark-matter density tends to be strongly peaked near the centres of these objects, and ANTARES has an excellent angular resolution, competitive limits can be set in the $E_{\mathrm{WIMP}} \gtrsim$ 50 GeV range where ANTARES is sensitive.

Limits on the spin-dependent (WIMP-proton) interaction cross section σ^p_{SD} from ANTARES observations of the Sun (left), and on the WIMP-WIMP velocity-averaged self-annihilation cross section $\sigma_A v$ from the Galactic Centre (right) using the $\tau\bar{\tau}$ channel are given in Fig. 12, and are described in further detail by C. Tönnis (ICRC2015 1207).

Dark-matter analyses by ANTARES also includes a search for a WIMP signature from the centre of the Earth (Gleixner & Tönnis, ICRC2015 1110), and a test of secluded dark-matter models in the Sun (Ardid & Tönnis, ICRC2015 1212).

ANTARES also places limits on beyond-the-standard-model physics, with searches for magnetic monopoles and nuclearites. Updates to existing limits are presented in Ref. El Bojaddaini & Păvălaş (ICRC2015 1060) and G. Păvălaş (ICRC2015 1060) respectively.

6. KM3NeT – ARCA and ORCA

KM3NeT (`www.km3net.org`) is a multi-site deep-sea research infrastructure. Two components are described here: ARCA (Astrophysical Research with Cosmics in the Abyss), a neutrino telescope for performing high-energy neutrino astronomy (P. Piattelli, ICRC2015 1158); and ORCA (Oscillations Research with Cosmics in the Abyss), to study neutrino oscillations parameters and resolve the neutrino mass hierarchy (J. Brunner, ICRC2015 1140).

ARCA will consist of two detection 'blocks', each consisting of 115 vertical detection units (DUs) with 18 multi-PMT digital optical modules (DOMs) with 31 photomultiplier tubes (PMTs) per DOM. A sketch of the ARCA block layout is given in Fig. 13 (left). Both blocks will be deployed 10 km apart at the KM3NeT Italian site (shore station at Capo Passero), with seafloor depth 3500 m, during Phase 2 of deployment. The KM3NeT-It site has been extensively studied in the context of the NEMO experiment (see e.g. Ref. [27]). ARCA is envisaged to be extended to a total of six blocks over multiple sites during Phase 3.

ORCA will consist of a single block with the same number of DUs and DOMs, but in a denser configuration (Fig. 13, middle). It will be fully deployed during Phase 2 at the KM3NeT France

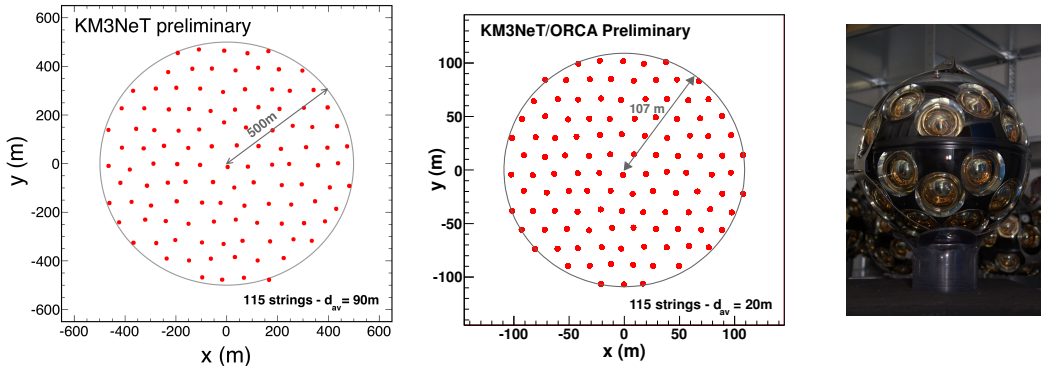

Figure 13: Preliminary seafloor layouts of the 115 detection units (DUs) in the ARCA (left) and ORCA (centre) blocks. Right: photograph of a KM3NeT DOM immediately after assembly.

site (seafloor depth 2475 m), 10 km East of the current ANTARES detector, with shore station at Lyon, France.

6.1 KM3NeT Phase 1: status

KM3NeT has completed its initial design and technical verification, and is currently in Phase 1 of production and deployment. Procedures for PMT testing (Mollo & Piattelli, ICRC2015 1159) and DU deployment (P. Kooijman, ICRC2015 1173) are in place, and timing (M. Bouwhuis, ICRC2015 1170), acoustic positional (S. Viola et al., ICRC2015 1169), and environmental (van Elewyck, Keller & Lindsey Clark, ICRC2015) calibration devices have been developed. A data-acquisition system (Biagi et al., ICRC2015 1172) based on the "all-data-to-shore" philosophy is in place at the KM3NeT-It site, while the main electro-optical cable and junction box have been deployed at KM3NeT-Fr.

Several stages of prototype DOMs have been deployed and tested, from an initial prototype DOM deployed at the ANTARES site in 2013, to a prototype detection unit with three DOMs at KM3NeT-It in 2014 (Biagi, Creusot, & Bormuth, ICRC2015 1164). The final design of the KM3NeT DOM is reported by Bruijn & van Eijk (ICRC2015 1157), and is the technology upon which both ORCA and ARCA is based.

A photograph of a KM3NeT DOM is given in Fig. 13 (right). The total effective area of the entire DOM is comparable to an ANTARES storey of three 10″ PMTs, but with a much more uniform angular coverage. Having many small co-located PMTs has several other advantages, including a large effective dynamic range, and the ability to calibrate on multi-fold coincidences from potassium 40 decays. Detailed GEANT simulations of the DOM are described in C. Hugon, ICRC2015 1106, and these are used as input to Monte Carlo simulations of the response of the prototype detection unit to background light and the atmospheric muon flux. Fig. 14 compares the results with data: it is evident that over the entire range, the prototypes are behaving as expected, and are well-modelled by the simulations.

The first full KM3NeT (ARCA) DU has recently been assembled and tested on-shore (A. Creusot, ICRC2015 1154), and is currently awaiting deployment at KM3NeT-It. KM3NeT Phase 1, which

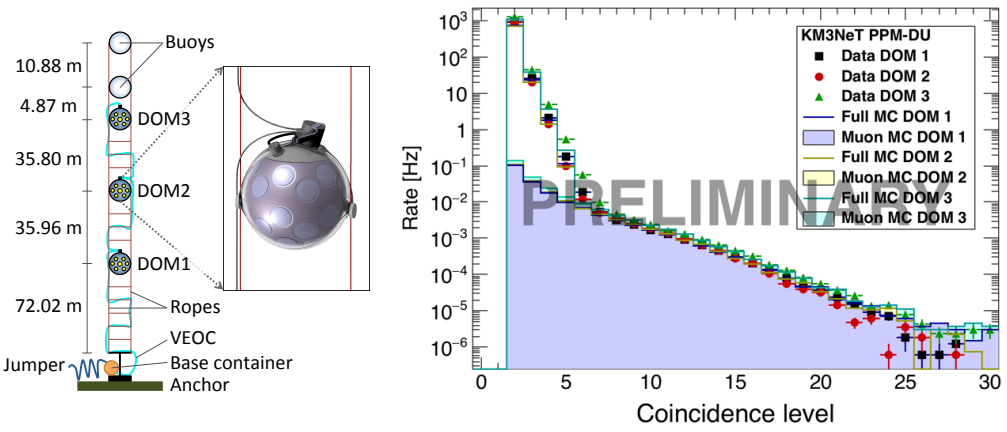

Figure 14: (From Biagi, Creusot, & Bormuth, ICRC2015 1164) Left: schematic diagram of the KM3NeT prototype detection unit deployed at KM3NeT-It, and Right: comparison of coincidence rates from data compared to Monte Carlo simulation. The second figure is an update to Fig. 4(a) from Biagi, Creusot, & Bormuth, after the cause of the excess of many-fold coincidences in simulations was discovered.

has now begun, will build and deploy 31 ARCA-scale DUs at KM3NeT-It, and 7 ORCA-scale DUs at KM3NeT-Fr, during 2015–2017. The rest of this contribution outlines the expected science potential of the Phase 2 instruments ARCA and ORCA, which are scheduled for completion as early as 2020.

6.2 ARCA

The main goal of ARCA is to perform high-energy neutrino astronomy. The total instrumented volume in Phase 2 will be comparable to that of the IceCube detector. It's northern latitude and excellent angular resolution will give it a superior sensitivity to southern and point-like sources, and hence ARCA will be ideally suited to identifying prospective Galactic sources of cosmic-ray acceleration, e.g. young supernova remnants such as RXJ 1713 [28], and pulsar wind nebula such as Vela X [29]. Further details of ARCA are given by P. Piattelli (ICRC2015 1158).

The expected reconstruction accuracies of muon track and cascade events in ARCA are described in Trovato, Drakopoulou & P. Sapienza (ICRC2015 1114) and D. Stransky et al. (ICRC2015 1108) respectively. The angular resolutions are shown in Fig. 15 after basic quality cuts. For the energy range above 30 TeV, the resolution is approximately 0.25° and 1.5° for ν_μ and ν_e CC events respectively.

The expected sensitivity of ARCA to astrophysical neutrino fluxes has been characterised by the sensitivity to point-like (Trovato & Barrios-Martí, ICRC2015 1113) and diffuse (Stransky, Coniglione & Fusco, ICRC2015 1107) sources in both the track and cascade channels. Several methods to discriminate against the atmospheric muon background have been developed, including the 'self-veto' effect [30] on downgoing atmospheric neutrinos (Heid, James & Pikounis, ICRC2015 1067). The estimated flux from generic E^{-2} point-like sources required for a 5 σ discovery as a function of their declination is compared to the discovery flux of IceCube, and limits from ANTARES, in Fig. 16 (left). Fig. 16 (right) shows the expected significance to a diffuse

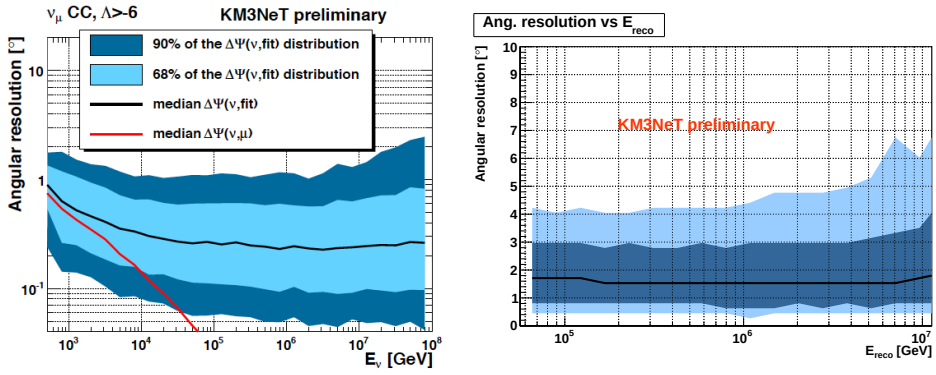

Figure 15: Angular resolutions of ARCA to (left) ν_μ and (right) ν_e CC events, showing the median (black lines), and 68% (inner shading) and 95% (outer shading) ranges, as a function of the neutrino energy.

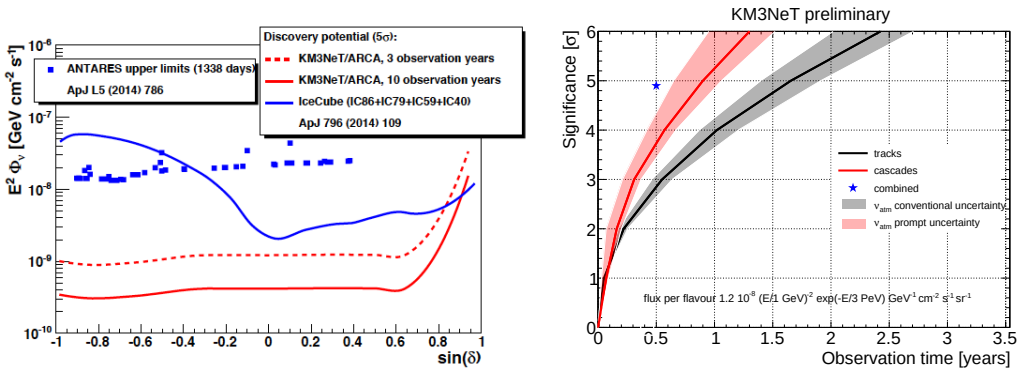

Figure 16: Left: ARCA 5 σ discovery flux to E^{-2} point-like sources of neutrinos after 3 and 10 years of operation (Trovato & Barrios-Martí, ICRC2015 1113), and Right: expected ARCA detection significance (Stransky, Coniglione & Fusco, ICRC2015 1107) as a function of time to the diffuse neutrino flux shown (c.f. Ref. [2]).

flux in both the track and cascade channels, as well as a preliminary estimate of their combined sensitivity.

6.3 ORCA

ORCA (Oscillations Research with Cosmic in the Abyss) will be a KM3NeT block in a dense configuration at the KM3NeT-Fr site near Toulon, and is described in detail by J. Brunner (ICRC2015 1140). As pointed out by Ref. [32], the effects of the specific values of neutrino oscillation parameters — particular ΔM_{23}, θ_{23}, $\delta_{\rm CP}$, and the neutrino mass hierarchy (NMH) itself — imprint themselves on the atmospheric neutrino flux in the few-GeV range. The goal of ORCA therefore is to study neutrino interactions in this range, and measure the zenith-angle and energy-dependence of the interaction rate for different interaction types — in particular, $\nu_e/\bar{\nu}_e$ and $\nu_\mu/\bar{\nu}_\mu$ CC interactions.

Extensive studies have been carried out on the ability of the ORCA baseline detector (Fig. 13, middle) to resolve the NMH, with intrinsic limits on reconstruction accuracy given by Hofestädt

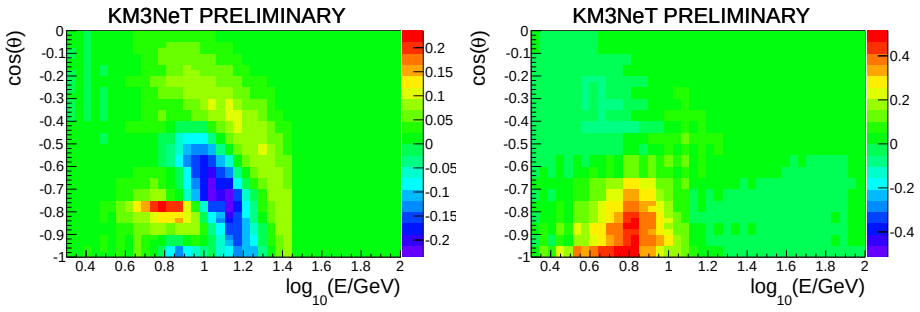

Figure 17: Mass hierarchy sensitivity ($|N_{\mathrm{NH}} - N_{\mathrm{IH}}|/\sqrt{N_{\mathrm{NH}}}$, where N is the number of events per bin after one year) showing the expected relative fluctuations in ν_μ CC (left) and ν_e CC (right), taking the resolution of ORCA into account (M. Jongen, ICRC2015 1092).

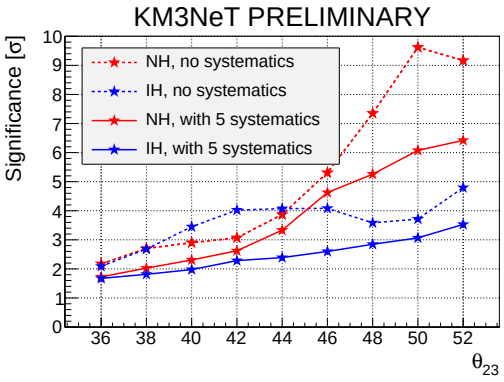

Figure 18: Expected sensitivity of ORCA to the neutrino mass hierarchy after 3 years of operation, both fitting for δ_{CP} and allowing it to take all values, and setting $\delta_{\mathrm{CP}} = 0$ (M. Jongen, ICRC2015 1092).

and James (ICRC2015 1084). The ability of ORCA to reconstruct track- and cascade-like events is described by S. Galatá (ICRC2015 1102) and J. Hofestädt (ICRC2015 1083) respectively, and atmospheric muon rejection is detailed in L.A. Fusco (ICRC2015 1072). Including these resolutions gives the hierarchy signature shown in Fig. 17.

The expected sensitivity of ORCA to the NMH after 3 years is given in Fig. 18 as a function of the experimental lifetime. The calculation, described in detail by M. Jongen (ICRC2015 1092), includes fitting for five systematic 'nuisance' parameters, as well as θ_{23}, and also indicate the effects of artificially setting $\delta_{\mathrm{CP}} = 0$ vs. including this in the fit. The ability to differentiate between hierarchies is dependent in particular upon the true value of θ_{23} and, to a lesser extent, δ_{CP}, whereas commonly $\delta_{\mathrm{CP}} = 0$ is assumed. A significance of 3σ is expected after three years.

7. Conclusion

The ANTARES neutrino telescope has proved itself to be a highly successful instrument for performing a wide range of physics analyses. In particular, its excellent angular resolution on both muon-track and cascade events, facilitated by the optical properties of deep-sea water, is well-suited to studying point-like sources of neutrinos. This capability has come to the fore now that an astrophysical neutrino flux has been detected by IceCube, and the key question now is: what

produces it? ANTARES has been able to limit a wide range of source scenarios, from galactic plane emission to blazars, and has performed the first point-source search using cascade events.

A new era in neutrino astronomy will begin in 2017, with the decommissioning of ANTARES, and the completion of KM3NeT Phase 1. The unique design of KM3NeT multi-PMT optical modules is expected to allow a very high resolution of neutrino interactions. The KM3NeT ORCA block will study the atmospheric flux in the 1–20 GeV range, and is expected in Phase 2 to determine the neutrino mass hierarchy to 3 σ significance in three years. In a sparser configuration at KM3NeT-It, ARCA in Phase 2 will be a similarly sized instrument to IceCube, but have a much-improved angular resolution. Eventually to reach 6 blocks during Phase 3, ARCA is optimised to study galactic sources of hadronic acceleration, and will study the astrophysical neutrino flux in unprecedented detail.

References

[1] M. Ageron et al., *Nuclear Instruments and Methods in Physics Research A* **656** (2011) 11.
[2] IceCube Collaboration, *Science* **342** (2013) 1242856.
[3] M. G. Aartsen, et al., *Phys. Rev. Lett.* **113** (2014) 101101.
[4] M. G. Aartsen et al., *ApJ* **809** (2015) 98.
[5] M. Spurio, *Phys. Rev. D* **90** (2014) 103004.
[6] S. Adrián-Martínez, et al., *ApJ* **786** (2014) L5.
[7] M. C. Gonzalez-Garcia, F. Halzen, and V. Niro, *Astroparticle Physics* **57** (014) 39.
[8] T. K. Gaisser, F. Halzen, and T. Stanev, *Phys. Rep.* **258** (1995) 173.
[9] W. B. Atwood et al., *ApJ* **697** (2009) 1071.
[10] F. Krauß et al., *A&A* **566** (2014) L7.
[11] S. Adrián-Martínez et al., *A&A* **576** (2015) L8.
[12] S. Adrián-Martínez et al., *Astroparticle Physics* **36** (2012) 204.
[13] E. Waxman and J. Bahcall, *Phys. Rev. Lett.* **78** (1997) 2292.
[14] S. Hümmer, M. Rüger, F. Spanier, and W. Winter, *ApJ* **721** (S2010) 630.
[15] S. Gao, K. Asano, and P. Mészáros, *J. Cosmology Astropart. Phys.* **11** (2012) 58.
[16] S. Adrián-Martínez et al., *A&A* **559** (2013) A9.
[17] M. Ageron et al., *Astroparticle Physics* **35** (2012) 530.
[18] M. Honda, T. Kajita, K. Kasahara, S. Midorikawa, and T. Sanuki, *Phys. Rev. D* **75** (2007) 043006.
[19] R. Enberg, M. H. Reno, and I. Sarcevic, *Phys. Rev. D* **78** (2008) 043005.
[20] J. A. Aguilar et al., *Physics Letters B* **696** (2011) 16.
[21] M. Su, T. R. Slatyer, and D. P. Finkbeiner, *ApJ* **724** (2010) 1044.
[22] S. Adrián-Martínez et al., *European Physical Journal C* **74** (2014) 2701.
[23] C. Lunardini, S. Razzaque, and L. Yang, *Phys. Rev. D* **92** (2015) 021301.
[24] A. Neronov, D. Semikoz, and C. Tchernin, *Phys. Rev. D* **89** (2014) 103002.
[25] D. Gaggero, D. Grasso, A. Marinelli, A. Urbano, and M. Valli, *ArXiv e-prints* `arXiv:1504.0022` (2015); PoS (ICRC2015) 489.
[26] M. Ackermann et al., *ApJ* **750** (2012) 3.
[27] S. Aiello et al., *Astroparticle Physics* **66** (2015) 1.
[28] S. R. Kelner, F. A. Aharonian, and V. V. Bugayov, *Phys. Rev. D* **74** (2006) 034018.
[29] F. Aharonian et al., *A&A* **448** (2006) L43.
[30] S. Schönert, T. K. Gaisser, E. Resconi, and O. Schulz, *Phys. Rev. D* **79** (2009) 043009.
[31] The IceCube-PINGU Collaboration, arXiv:1401.2046 (2014).
[32] E. K. Akhmedov, S. Razzaque, and A. Y. Smirnov, *Journal of High Energy Physics* **2** (2013) 82.